Nonlinear Optomechanically Induced Transparency in a Spinning Kerr Resonator

Ya-Jing Jiang(蒋亚静)[1], Xing-Dong Zhao(赵兴东)[1*], Shi-Qiang Xia(夏世强)[1*], Chun-Jie Yang(杨春洁)[1*], Wu-Ming Liu(刘伍明)[2], and Zun-Lue Zhu(朱遵略)[1]

[1]*School of Physics, Henan Normal University, Xinxiang 453007, China*
[2]*Beijing National Laboratory for Condensed Matter Physics, Institute of Physics, Chinese Academy of Sciences, Beijing 100190, China*

(Received 21 September 2022; accepted manuscript online 21 November 2022)

We theoretically study optomechanically induced transparency in a spinning Kerr-nonlinear resonator. The interplay between the optical Kerr effect and the Sagnac effect provides a flexible tool for modifying the optomechanically induced transparency windows of the signal comparing to the system of a single spinning resonator. It is found that the system will exhibit distinct transparency phenomenon and fast-to-slow light effects. More importantly, a symmetric transparency window appears by adjusting the rotation-induced Sagnac frequency shift to compensate for the Kerr-induced frequency shift. These results open up a new way to explore novel light propagation of optomechanically induced transparency devices in spinning resonators with Kerr nonlinearity.

DOI: 10.1088/0256-307X/39/12/124202

Cavity optomechanics have attracted increasing attention in recent years,[1,2] which enables a variety of important applications, including highly sensitive sensors,[3–6] quantum state transducers,[7,8] coherent phonon lasing or transport,[9–12] and generation of non-classical states of light and mechanical motion.[13,14] As an example closely related to this present work, optomechanically induced transparency (OMIT) has been studied in a variety of systems,[15–24] also many interesting effects related to OMIT have been revealed, such as high-order sidebands[25,26] and cascade optical transparency.[27] These advances provide versatile platforms to coherently control light propagation in optomechanical devices, such as nonreciprocal optical devices[28–31] and optical wavelength conversion.[32,33]

On the other hand, whispering-gallery-mode (WGM) resonators with high quality factor have been a promising candidate for exploring quantum science and technology,[34,35] which have already been used in a wide range of areas, e.g., cavity quantum electrodynamics,[36–38] optical filtering,[39] and highly sensitive detection.[40–43] Due to the long photon lifetime and small mode volume, WGM resonators have a high intracavity field intensity and the enhanced effective nonlinearity,[35,44,45] therefore leading to a lot of applications such as Raman laser,[46] optical frequency comb generation,[47,48] nonlinear frequency conversion,[49,50] and chiral devices.[51] In particular, an asymmetric transparency dip of OMIT in a single Kerr resonator has been observed in the recent experiment, which can be tuned to be a symmetric transparency window by appropriately varying the pump frequency.[20] Furthermore, high-order sidebands and the corresponding group delays have also been studied theoretically,[52] providing a new method to tuning light propagation in nonlinear resonators.

Very recently, spinning optical devices have become a versatile platform to explore quantum optics. In a rotating device, the clockwise (CW) and the counterclockwise (CCW) optical modes experience different frequency shifts. This phenomenon, known as the Sagnac effect,[53,54] is used for sensitive measurements of the angular velocity of the medium.[55] Many exotic effects have been revealed in rotating optical systems, such as mode coupling,[56] nonreciprocal optical solitons,[57] chiral symmetry breaking,[58] and nonlinear anti-parity-time gyroscope.[59] It also shows that nonreciprocal light transmission can be achieved in a spinning WGM resonator, without any magnetic field or optical nonlinearity.[60] Spinning optical devices can also be used in nonreciprocal phonon transport,[61] nanoparticle sensing,[62,63] nonreciprocal photon blockade,[64–67] and nonreciprocal quantum entanglement.[68] We also note that both the OMIT and group delay have already been studied in a rotating microresonator, where the rotation provides a new degree of freedom and induces richer phenomena.[69–71] However, the intrinsic nonlinearity of WGM resonators has been neglected in these works, which needs to be further investigated in our system, for example, the Kerr nonlinearity interaction can be compensated or tuned by spinning the resonators.

In this work, we study the impact of the Kerr nonlinearity on the OMIT in a spinning WGM resonator. We show that both the transmission rate and the group delay of the probe light can be tuned by steering the Kerr coefficient. Nonreciprocal light propagation can be realized by tuning the rotation speed and the probe detuning. We also find that a symmetric transparency window can be achieved by adjusting the Kerr-induced frequency shift to compensate for the Sagnac-induced frequency shift. Our work provides a practical and sensitive way to control light propagation in nonlinear resonators.

As shown in Fig. 1, we consider a nonlinear spherical microresonator coupled to a tapered fiber. The resonator, with resonant frequency ω_c and intrinsic optical damping

*Corresponding authors. Email: phyzhxd@gmail.com; xiashiqiang@htu.edu.cn; yangchj@hotmail.com
© 2022 Chinese Physical Society and IOP Publishing Ltd

rate γ_0, is driven by a strong pump light at frequency $\omega_{\rm L}$ and a weak probe light at frequency $\omega_{\rm p}$. The amplitudes of the pump and probe fields are $\varepsilon_{\rm L} = \sqrt{\gamma_{\rm ex} P_{\rm L}/\hbar\omega_{\rm L}}$ and $\varepsilon_{\rm p} = \sqrt{\gamma_{\rm ex} P_{\rm p}/\hbar\omega_{\rm p}}$, respectively, where $P_{\rm L}$ or $P_{\rm p}$ are the pump or probe power, and $\gamma_{\rm ex}$ is the damping rate of the resonator to the fiber. The resonator, supporting a mechanical breathing mode with frequency $\omega_{\rm m}$ and effective mass $m_{\rm eff}$, spins with the rotation speed Ω, and is positioned near a stationary waveguide. We note that such a system has been experimentally performed by Maayani *et al.*[60] By mounting a spherical resonator on a turbine and positioning the spinning silica sphere near a single-mode fiber, the light is coupled into or out of the resonator evanescently through the tapered region of the fiber. The position of the fiber can be self-adjusted, leading to a stable resonator-fiber coupling. In this experiment the taper does not touch or stick to the resonator even if the taper is pushed toward it.

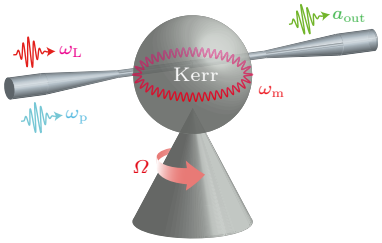

Fig. 1. Schematic illustration of a spinning resonator made of a Kerr-nonlinear material. The resonator, supporting a mechanical mode with frequency $\omega_{\rm m}$ and effective mass $m_{\rm eff}$, is driven by a strong pump field at frequency $\omega_{\rm L}$ and a weak probe field at frequency $\omega_{\rm p}$. The rotation speed is denoted as Ω.

Meanwhile, we know that third-order nonlinear susceptibility is the lowest-order nonlinearity in the optical domain for materials with central symmetry (for example, fused silica), and can be characterized by the Kerr nonlinearity,[48]

$$U = \frac{\hbar\omega_{\rm c}^2 c n_2}{n_0^2 V_{\rm eff}}, \tag{1}$$

where n_0 is the linear refractive index, and c is the speed of light in vacuum. The nonlinear refractive index n_2 is associated with the third-order nonlinear optical susceptibility $\chi^{(3)}$,

$$n_2 = \frac{3}{4 n_0^2 \epsilon_0 c}\chi^{(3)}, \tag{2}$$

with ϵ_0 being the vacuum permittivity. In microresonators, the typical values of n_0, n_2, and $\chi^{(3)}$ are $1.4 \lesssim n_0 \lesssim 3.4$, $10^{-20} \lesssim n_2 \lesssim 10^{-17}\,{\rm m}^2/{\rm W}$, and $10^{-23} \lesssim \chi^{(3)} \lesssim 10^{-18}\,{\rm m}^2/{\rm V}^2$.[72] The refractive index n can be written as $n = n_0 + n_2 I$, where I denotes the time-averaged intensity of the optical field. $V_{\rm eff}$ is the effective mode volume of the microsphere, which can be estimated with[44]

$$\begin{aligned} V_{\rm eff} &\approx \frac{(\int \boldsymbol{E}^2 d^3\boldsymbol{r})^2}{\int \boldsymbol{E}^2\boldsymbol{E}^2 d^3\boldsymbol{r}} \\ &\approx 3.4\pi^{3/2}\Big(\frac{\lambda}{2\pi n_0}\Big)^3 l^{11/6}\sqrt{l-m+1}, \end{aligned} \tag{3}$$

where $\boldsymbol{E}$ and λ are the electric field and wavelength of the optical mode, respectively. The integers l and m are the angular momentum and the azimuthal mode number, respectively, which satisfy $l \approx 2\pi n r/\lambda$ and $m \leqslant |l|$.[44] Here, r is the radius of the spherical resonator.

By spinning the resonator, the refractive indices of the CW and CCW optical modes are modified as $n_\pm = n[1 \pm R\Omega(n^{-2}-1)/c]$,[60] which lead to a frequency shift due to the Sagnac effect,[73] i.e., $\omega_{\rm c} \to \omega_{\rm c} \pm \Delta_{\rm Sag}$, with

$$\Delta_{\rm Sag} = \frac{n r \Omega \omega_{\rm c}}{c}\Big(1 - \frac{1}{n^2} - \frac{\lambda}{n}\frac{dn}{d\lambda}\Big). \tag{4}$$

The dispersion term $\lambda dn/nd\lambda$, characterizing the relativistic origin of the Sagnac effect, is typically small and can be safely ignored.[60]

In rotation frame at frequency $\omega_{\rm L}$, the Hamiltonian of the system can be written as ($\hbar = 1$)

$$\begin{aligned} H &= H_0 + H_{\rm int} + H_{\rm dr}, \\ H_0 &= (\Delta_{\rm c} - \Delta_{\rm Sag})a^\dagger a + \frac{p^2}{2m_{\rm eff}} + \frac{1}{2}m_{\rm eff}\omega_{\rm m}^2 x^2 + \frac{p_\theta^2}{2m_{\rm eff}r^2}, \\ H_{\rm int} &= -gxa^\dagger a + Ua^\dagger a^\dagger aa, \\ H_{\rm dr} &= i\varepsilon_{\rm L}(a^\dagger - a) + i\varepsilon_{\rm p}(a^\dagger e^{-i\xi t} - ae^{i\xi t}), \end{aligned} \tag{5}$$

where $\Delta_{\rm c} = \omega_{\rm c} - \omega_{\rm L}$ is the resonator-pump detuning, $\xi = \omega_{\rm p} - \omega_{\rm L}$ is the probe-pump detuning, $g = \omega_{\rm c}/r$ is the optomechanical coupling strength, a is the optical annihilation operator, x, p and θ, p_θ are the displacement, momentum and the rotation angle, angular momentum operators,[69] respectively, which satisfy the commutation relations $[x,p] = [\theta, p_\theta] = i$.

We have the evolution equations

$$\begin{aligned} \dot{a} =& -(i\Delta_{\rm c} - i\Delta_{\rm Sag} - igx + \gamma)a - 2iUa^\dagger a^2 \\ &+ \varepsilon_{\rm L} + \varepsilon_{\rm p}e^{-i\xi t}, \\ \ddot{x} =& -\gamma_{\rm m}\dot{x} - \omega_{\rm m}^2 x + \frac{g}{m_{\rm eff}}a^\dagger a + \frac{p_\theta^2}{m_{\rm eff}^2 r^3}, \\ \dot{\theta} =& \frac{p_\theta}{m_{\rm eff}r^2}, \\ \dot{p}_\theta =& 0, \end{aligned} \tag{6}$$

where $\gamma = (\gamma_0 + \gamma_{\rm ex})/2$ is the total optical loss, and $\gamma_{\rm m}$ is the mechanical damping rate. In order to solve the intracavity field and mechanical displacement, we write each operator as the sum of its steady value and a small fluctuation, i.e., $a = a_{\rm s} + \delta a$ and $x = x_{\rm s} + \delta x$. The steady-state values can be obtained as

$$\begin{aligned} a_{\rm s} &= \frac{\varepsilon_{\rm L}}{i(\Delta_{\rm c} - \Delta_{\rm Sag}) - igx_{\rm s} + \gamma + 2iU|a_{\rm s}|^2}, \\ x_{\rm s} &= \frac{g}{m_{\rm eff}\omega_{\rm m}^2}|a_{\rm s}|^2 + r\Big(\frac{\Omega}{\omega_{\rm m}}\Big)^2, \end{aligned} \tag{7}$$

where $\Omega = \dot{\theta}$ is the rotation speed. We can see that both the Kerr nonlinearity and the rotation have an effect on the values of the mechanical displacement $x_{\rm s}$ and the intracavity optical amplitude $a_{\rm s}$. This means that the effective optomechanical coupling and the breathing-mode oscillations can be tuned by the two effects, which in turn result in modified OMIT properties of the system. Likewise, the fluctuation terms satisfy the equations

$$\begin{aligned} \delta\dot{a} =& -[i(\Delta_{\rm c} - \Delta_{\rm Sag}) - igx_{\rm s} + \gamma + 4iU|a_{\rm s}|^2]\delta a + iga_{\rm s}\delta x \\ &- 2iUa_{\rm s}^2\delta a^* + \varepsilon_{\rm p}e^{-i\xi t}, \\ \delta\ddot{x} + &\gamma_{\rm m}\delta\dot{x} + \omega_{\rm m}^2\delta x = \frac{g}{m}(a_{\rm s}^*\delta a + a_{\rm s}\delta a^*). \end{aligned} \tag{8}$$

Then writing the fluctuation terms in the following forms:

$$\delta a = A_- e^{-i\xi t} + A_+ e^{i\xi t},$$
$$\delta x = X e^{-i\xi t} + X^* e^{i\xi t}, \tag{9}$$

and substituting Eq. (9) into Eq. (8), we obtain

$$\begin{aligned}
&[-i\xi + i(\Delta_c - \Delta_{Sag} - g x_s + 4U|a_s|^2) + \gamma]A_- \\
&= iga_s X - 2iUa_s^2 A_+^* + \varepsilon_p, \\
&[-i\xi - i(\Delta_c - \Delta_{Sag} - g x_s + 4U|a_s|^2) + \gamma]A_+^* \\
&= -iga_s^* X + 2iU(a_s^*)^2 A_-, \\
&(-\xi^2 - i\xi\gamma_m + \omega_m^2)X = \frac{g}{m_{eff}}(a_s^* A_- + a_s A_+^*).
\end{aligned} \tag{10}$$

Solving Eq. (10) leads to

$$\begin{aligned}
A_- = &[(\mu_- + i\eta g^2|a_s|^2)\varepsilon_p]/[\mu_+\mu_- - 2\eta g^2|a_s|^2(\Delta_c - \Delta_{Sag} \\
&- g x_s + 2U|a_s|^2) - 4U^2|a_s|^4],
\end{aligned} \tag{11}$$

with

$$\begin{aligned}
\mu_\pm &= -i\xi + \gamma \pm i(\Delta_c - \Delta_{Sag} - g x_s + 4U|a_s|^2), \\
\eta &= [m_{eff}(\omega_m^2 - i\gamma_m\xi - \xi^2)]^{-1}.
\end{aligned} \tag{12}$$

The expectation value of the output field can be calculated by using the input–output relation,[74]

$$a_{out} = a_{in} - \sqrt{\gamma_{ex}} A_-, \tag{13}$$

where a_{in} and a_{out} are the input and output field operators, respectively. Then the transmission rate and reflectivity of the probe field are derived as follows:

$$\begin{aligned}
T = |t_p|^2 &= \left|\frac{a_{out}}{a_{in}}\right|^2 = \left|1 - \frac{\gamma_{ex}}{\varepsilon_p} A_-\right|^2, \\
R &= \left|\frac{a_{out} - a_{in}}{a_{in}}\right|^2 = \left|\frac{\gamma_{ex}}{\varepsilon_p} A_-\right|^2.
\end{aligned} \tag{14}$$

This sets up the framework for our discussion of the role of the Kerr nonlinearity and the rotation on the transmission rate and the group delay of the probe field.

In the work, we use experimentally feasible parameters,[45,48,75] i.e., $n = 1.44$, $n_2 = 2.2\times10^{-20}\,\mathrm{m^2/W}$, $r = 0.25\,\mathrm{mm}$, $\lambda = 1.55\,\mu\mathrm{m}$, $\gamma_0 = \gamma_{ex} = 6.43\,\mathrm{MHz}$, $\Delta_c = \omega_m$, $m_{eff} = 2\,\mu\mathrm{g}$, $\omega_m = 200\,\mathrm{MHz}$, and $\gamma_m = 0.2\,\mathrm{MHz}$. The Kerr nonlinearity can be tuned by choosing an appropriate driving laser mode. For example, we can estimate the minimum of the effective mode volume V_{eff} as $6\times10^4\,\mu\mathrm{m}^3$ if we set $l = m$ in Eq. (3), which leads to a maximum value of the Kerr-nonlinear coefficient as $U_{max} = 0.2\,\mathrm{mHz}$. Furthermore, we note that the rotation speed of a spherical resonator with $r = 1.1\,\mathrm{mm}$ can be up to 6.6 kHz in experiment.[60] As the maximum of the rotation speed is proportional to r^{-2} with the fixed driving power, the smaller the resonator, the higher the rotation speed of the spinnor. In consideration of these factors, the rotation speed is not more than 120 kHz in our calculations.

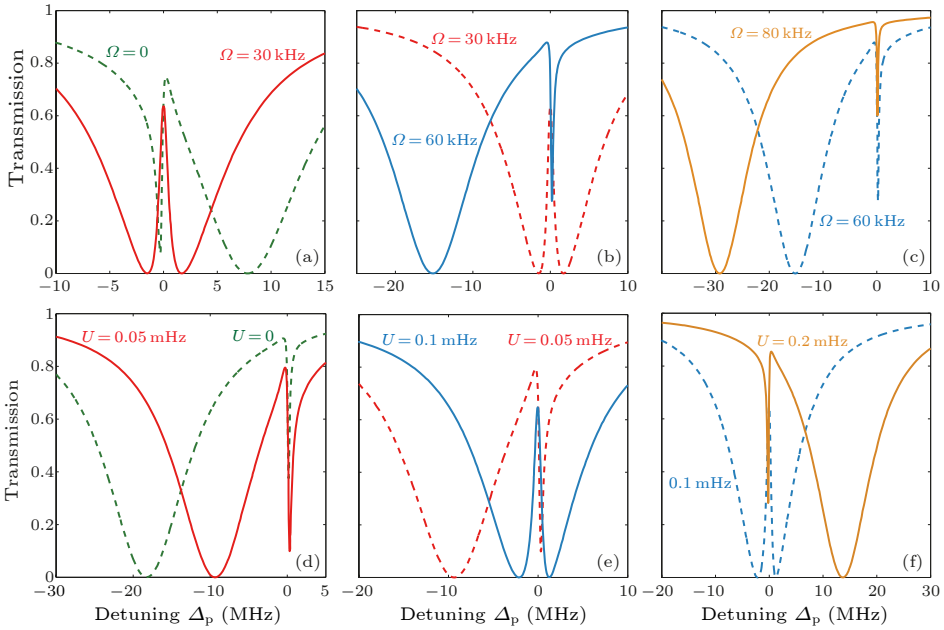

Fig. 2. Transmission rate T of the probe field as a function of the probe-resonator detuning Δ_p. We choose $U = 0.05\,\mathrm{mHz}$ in (a)–(c), $\Omega = 50\,\mathrm{kHz}$ in (d)–(f), and $P_L = 5\,\mathrm{W}$ in (a)–(f).

Firstly, we are interested in the impact of the Kerr and rotation on the transmission spectrum. Figures 2(a)–2(c) show the transmission rate T as a function of the probe-resonator detuning $\Delta_p = \omega_p - \omega_c$ by varying different rotation rates and fixing the Kerr nonlinearity U at 0.05 mHz. For the optomechanical Kerr resonator without spinning, we note that the transmission spectrum is asymmetric and the OMIT peak located around the resonator detuning of $\Delta_p = 0$. As we know from Ref. [15], the linewidth of the OMIT window is $\gamma_m + g^2|a_s|^2/\gamma m_{eff}^2\omega_m^2$. Moreover, the values of transmission peaks and the separation between the two tips (two lowest T values) on each side of peak decrease at first, then increase by varying the spinning speed Ω [$T_p = 0.75$, $T_p = 0.64$ and $T_p = 0.87$ for $\Omega = 0$, $\Omega = 30\,\mathrm{kHz}$ and $\Omega = 60\,\mathrm{kHz}$, respectively. See Figs. 2(a) and 2(b)]. In this case, the Kerr-induced frequency shift

can be estimated with [20]

$$\Delta\omega = 2U|a_s|^2 \approx \frac{2\omega_c c n_2}{n_0^2 V_{\rm eff}} \cdot \frac{\gamma}{(\Delta_c - \Delta_{\rm Sag})^2 + \gamma^2} \cdot P_L. \quad (15)$$

The numerical result indicates $\Delta\omega \approx 3.8\,\text{MHz}$ for $\Omega = 0$, and an absorption dip appears at $\Delta_p \approx 2\Delta\omega$ [see Fig. 2(a)]. Much more interestingly, we also notice the emergence of a symmetric transparency window around $\Delta_p = 0$ at $\Omega = 30\,\text{kHz}$, which cannot be observed in a single Kerr or spinning resonator, and it comes from an exact balance between the Sagnac effect and the Kerr nonlinear effect. More specifically, the frequency shift induced by the Kerr effect is compensated for by the Sagnac effect. In this case, the effective detuning

$$\Delta_{\rm eff} = \Delta_c - g x_s - \Delta_{\rm Sag} + 2\Delta\omega \approx \omega_m \quad (16)$$

can lead to an enhanced optomechanical interaction. By increasing the rotation speed further, the Sagnac effect dominates over the Kerr effect, and a strong absorption dip is observed in $\Delta_p < 0$ region as shown in Fig. 2(c).

Further, in order to study the impact of Kerr effect on the transmission spectrum, we plot the transmission rate in Figs. 2(d)–2(f) with a variance of the Kerr nonlinearity and fixing $\Omega = 50\,\text{kHz}$. As can be seen, without the Kerr effect ($U = 0$), an obvious absorption dip appears in the $\Delta_p < 0$ regime. The increasing Kerr nonlinearity leads to a blue shift of the absorption frequency, and the absorption frequency can even be extended to $\Delta_p > 0$ regime. For comparison, we know that the OMIT peaks stay always at the resonance point $\Delta_p \approx 0$, and an absorption dip always emerges in the Fano-like spectrum for a large nonlinearity in a Kerr resonator (no spinning). When considering rotation, the width of the transmission peak at $\Delta_p \approx 0$ changes by increasing the optical nonlinearity. Once the Kerr effect dominates over the Sagnac effect in the frequency shift process, the absorption dip can also be tuned from the red detuning region to the blue detuning region, and its location depends on the relative values of the frequency shifts induced by the Sagnac effect and the Kerr nonlinearity. Note that, in compensation with the Sagnac effect, a symmetric transmission spectrum is constructed again with the absorption frequency located at $\Delta_p \approx 0$. We can see that the Kerr nonlinearity has a significant impact on the optical transmission in a spinning resonator. These results indicate that the transmission rate of the signal light can be adjusted conveniently by changing the rotation speed or the Kerr nonlinearity of the resonator, which is obviously different from that of a spinning resonator or Kerr resonator.

As we know, for the familiar stationary resonator with negligible optical nonlinearity, there is a transparency peak located at the $\Delta_p = 0$, with two symmetric absorption sidebands in the non-resonant region. Studies indicate that the locations of the transparency window and absorption sidebands can be changed by spinning the resonator or steering the optical nonlinearity. [62,70] However, the impact of the rotation direction on the light propagation in a nonlinear Kerr resonator has not been studied before. In Figs. 3(a)–3(c), we focus on the features of the transmission spectrum with a change of the spinning direction ($\Omega > 0$ corresponding to counterclockwise and $\Omega < 0$ corresponding to clockwise rotation, with $U = 0.2\,\text{mHz}$). Obviously, the frequency shift of the Fano-like transmission spectrum is associated with the rotation directions and is about $g x_s \pm \Delta_{\rm Sag} - 2\Delta\omega$, where $\pm$ denotes $\Omega > 0$ or $\Omega < 0$. It indicates that the rotation direction provides another degree of freedom for the manipulation of the transmission spectrum.

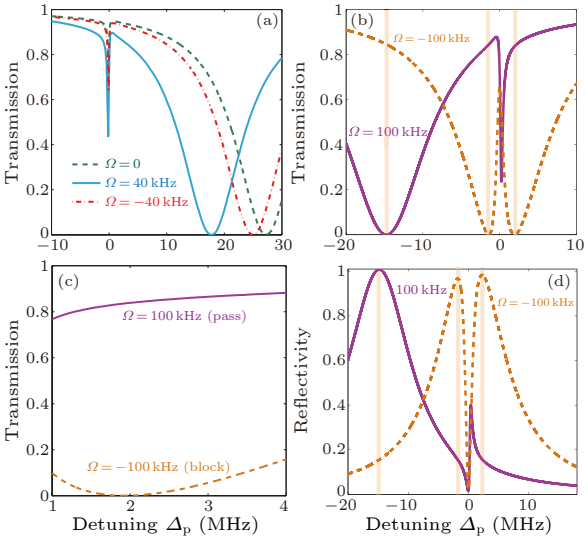

Fig. 3. Transmission rate T (a)–(c) and reflectivity R (d) of the probe field as a function of the probe-resonator detuning Δ_p for different values of rotation speed Ω with $U = 0.2\,\text{mHz}$. We set $P_L = 5\,\text{W}$ in (a)–(d).

More distinct transmission features can be observed for a higher rotation speed, as shown in Fig. 3(b). Clearly, a symmetry spectrum is reconstructed in $\Omega = -100\,\text{kHz}$, which is associated with the compensation of the frequency shifts induced by the Kerr nonlinearity and Sagnac effect. In contrast, much more prominent asymmetry is observed when $\Omega = 100\,\text{kHz}$. It results from the synergic actions of the Kerr and Sagnac effect: the former leads to a red shift of the frequency, as well as the other one. In addition, we also find the existence of nonreciprocal transparency windows, [70] as shown by the vertical yellow bands in Fig. 3(b). At $\Delta_p \approx 2\,\text{MHz}$, the probe light can be transmitted ($T(\Omega > 0) \approx 0.85$) or blocked ($T(\Omega < 0) \approx 0$) with the counterclockwise or clockwise rotation of the spinnor in Fig. 3(c). However, at $\Delta_p \approx -14.5\,\text{MHz}$, the situation is inversed. More interestingly, the nonreciprocal window appears around the transparency peak, where the optomechanical coupling is strong. Thus, it is the strong optomechanical interaction that leads to significantly different new features in the transmission spectrum. Noticeably, our results also indicate that the optical nonreciprocity can be realized flexibly by tuning both the optical nonlinearity and rotation speed. For completeness, the reflectivity of the probe light is plotted in Fig. 3(d). Nonreciprocal reflection can be observed with a high rotation speed, which is in accordance with the transmission spectrum as shown in Fig. 3(b).

Finally, we study the slow and fast light effect in this spinning Kerr system, which can be characterized by the optical group delay:

$$\tau_g = \frac{d\arg(t_p)}{d\Delta_p}. \quad (17)$$

Figure 4(a) shows that the group delay τ_g can be well tuned by adjusting the Kerr coefficient U or the pump power P_L at the fixed rotation speed $\Omega = 40\,\text{kHz}$. Both the slow light ($\tau_g > 0$) and fast light ($\tau_g < 0$) can be found. It indicates that a slow-to-fast light switch can be realized with a change of the pumping power. Meanwhile, the maximum value of the group delay is increased with an enhancement of the Kerr nonlinearity, which mean that the slow light phenomenon is enhanced. For example, $\tau_{g,\max} \approx 1.2\,\mu\text{s}$ for $U = 0$ and $\tau_{g,\max} \approx 3.7\,\mu\text{s}$ for $U = 0.2\,\text{mHz}$. This is the fact that frequency shifts induced by the Kerr nonlinearity and the Sagnac effect result in an enhanced effective optomechanical interaction. Figure 4(b) shows the dependence of the group delay on both the rotation speed and the Kerr coefficient. For $U = 0$, τ_g decreases with a higher rotation speed. For other parts, the relation between τ_g and the rotation speed Ω is nonlinear. To achieve a larger group delay, the rotation speed and Kerr nonlinearity should be chosen carefully. Our scheme provides additional control of the light propagation in nonlinear resonators by using the optical Sagnac effect.

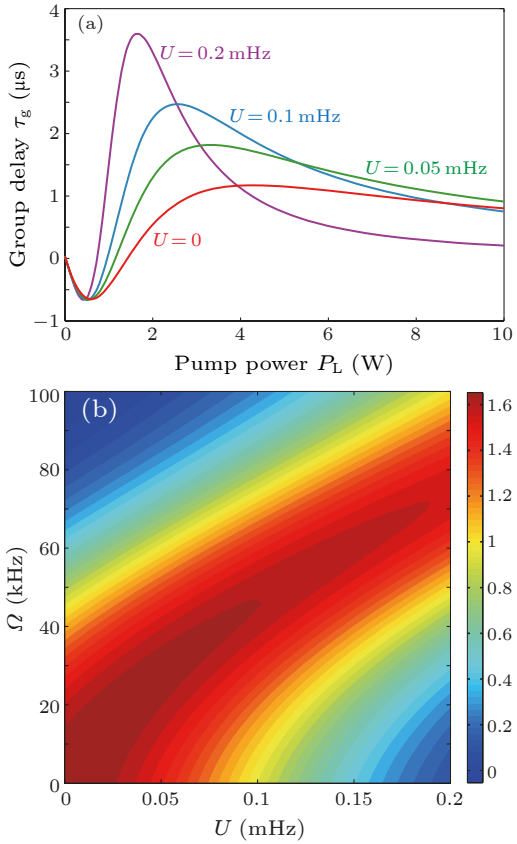

Fig. 4. Group delay of the probe light τ_g: (a) group delay as a function of the pump power P_L with a fixed $\Omega = 40\,\text{kHz}$, (b) group delay as functions of the rotation speed Ω and the Kerr coefficient U with a fixed $P_L = 5\,\text{W}$. We set $\Delta_p = 0$ in both (a) and (b).

We have studied OMIT in a spinning optomechanical resonator with Kerr nonlinearity. In such a system, the presence of the Kerr nonlinearity and Sagnac effect induce frequency shifts of the probe light, which influence the intracavity optical intensity as well as the mechanical displacement. This leads to modified properties of OMIT including the transmission rate and group delay. Nonreciprocal light propagation can also be realized. In particular, a symmetric OMIT spectrum can be reconstructed if the Kerr-induced frequency shift compensates for the Sagnac-induced shift. We note that the rotation speed of a nanoobject can be extended to the GHz regime in very recent experiments,[76,77] which can be further considered in optomechanical systems to explore new effects. Our work can also be extended to coupled nonlinear resonators or resonators coupled with nanoparticles,[43] which can be used for other applications in optoacoustic devices,[78] chiral sensors,[79] and topological optomechanical effects.[80,81]

Acknowledgement. This work was supported by the Doctoral Scientific Research Foundation of Henan Normal University (Grant No. 20210397), the Henan Province Key Scientific Research Project Plan of Colleges and Universities (Grant No. 23A140001), the National Natural Science Foundation of China (Grant Nos. 11704103, 12074106, 61835013, and 12074105), and the National Key R&D Program of China (Grant Nos. 2021YFA1400900, 2021YFA0718300, and 2021YFA1400243).

References

[1] Aspelmeyer M, Kippenberg T J, and Marquardt F 2014 *Rev. Mod. Phys.* **86** 1391
[2] Metcalfe M 2014 *Appl. Phys. Rev.* **1** 031105
[3] Arcizet O, Cohadon P F, Briant T, Pinard M, Heidmann A, Mackowski J M, Michel C, Pinard L, Français O, and Rousseau L 2006 *Phys. Rev. Lett.* **97** 133601
[4] Gavartin E, Verlot P, and Kippenberg T J 2012 *Nat. Nanotechnol.* **7** 509
[5] Rashid M, Toroš M, Setter A, and Ulbricht H 2018 *Phys. Rev. Lett.* **121** 253601
[6] Zhao W, Zhang S D, Miranowicz A, Jing H 2020 *Sci. Chin. Phys. Mech. Astron.* **63** 224211
[7] Bagci T, Simonsen A, Schmid S, Villanueva L G, Zeuthen E, Appel J, Taylor J M, Sørensen A, Usami K, Schliesser A, and Polzik E S 2014 *Nature* **507** 81
[8] Lecocq F, Clark J B, Simmonds R W, Aumentado J, and Teufel J D 2016 *Phys. Rev. Lett.* **116** 043601
[9] Grudinin I S, Lee H, Painter O, and Vahala K J 2010 *Phys. Rev. Lett.* **104** 083901
[10] Jing H, Özdemir Ş K, Lü X Y, Zhang J, Yang L, and Nori F 2014 *Phys. Rev. Lett.* **113** 053604
[11] Kim S, Xu X, Taylor J M, and Bahl G 2017 *Nat. Commun.* **8** 205
[12] Zhang J, Peng B, Özdemir Ş K, Pichler K, Krimer D O, Zhao G, Nori F, Liu Y X, Rotter S, and Yang L 2018 *Nat. Photon.* **12** 479
[13] Wollman E E, Lei C U, Weinstein A J, Suh J, Kronwald A, Marquardt F, Clerk A A, and Schwab K C 2015 *Science* **349** 952
[14] Riedinger R, Hong S, Norte R A, Slater J A, Shang J, Krause A G, Anant V, Aspelmeyer M, and Gröblacher S 2016 *Nature* **530** 313
[15] Weis S, Rivière R, Deléglise S, Gavartin E, Arcizet O, Schliesser A, and Kippenberg T J 2010 *Science* **330** 1520
[16] Safavi-Naeini A H, Mayer Alegre T P, Chan J, Eichenfield M, Winger M, Lin Q, Hill J T, Chang D E, and Painter O 2011 *Nature* **472** 69
[17] Zhou X, Hocke F, Schliesser A, Marx A, Huebl H, Gross R, and Kippenberg T J 2013 *Nat. Phys.* **9** 179
[18] Kronwald A and Marquardt F 2013 *Phys. Rev. Lett.* **111** 133601
[19] Jing H, Özdemir Ş K, Geng Z, Zhang J, Lü X Y, Peng B, Yang L, and Nori F 2015 *Sci. Rep.* **5** 9663

[20] Shen Z, Dong C H, Chen Y, Xiao Y F, Sun F W, and Guo G C 2016 *Opt. Lett.* **41** 1249

[21] Lü H, Wang C Q, Yang L, and Jing H 2018 *Phys. Rev. Appl.* **10** 014006

[22] Zhang H, Saif F, Jiao Y, and Jing H 2018 *Opt. Express* **26** 25199

[23] Lu T X, Jiao Y F, Zhang H L, Saif F, and Jing H 2019 *Phys. Rev. A* **100** 013813

[24] Bodiya T, Sudhir V, Wipf C, Smith N, Buikema A, Kontos A, Yu H, and Mavalvala N 2019 *Phys. Rev. A* **100** 013853

[25] Xiong H, Si L G, Zheng A S, Yang X, and Wu Y 2012 *Phys. Rev. A* **86** 013815

[26] Jiao Y, Lü H, Qian J, Li Y, and Jing H 2016 *New J. Phys.* **18** 083034

[27] Fan L, Fong K Y, Poot M, and Tang H X 2015 *Nat. Commun.* **6** 5850

[28] Shen Z, Zhang Y L, Chen Y, Zou C L, Xiao Y F, Zou X B, Sun F W, Guo G C, and Dong C H 2016 *Nat. Photon.* **10** 657

[29] Fang K, Luo J, Metelmann A, Matheny M H, Marquardt F, Clerk A A, and Painter O 2017 *Nat. Phys.* **13** 465

[30] Verhagen E and Alù A 2017 *Nat. Phys.* **13** 922

[31] Shen Z, Zhang Y L, Chen Y, Sun F W, Zou X B, Guo G C, Zou C L, and Dong C H 2018 *Nat. Commun.* **9** 1797

[32] Hill J T, Safavi-Naeini A H, Chan J, and Painter O 2012 *Nat. Commun.* **3** 1196

[33] Liu Y X, Davanço M, Aksyuk V, and Srinivasan K 2013 *Phys. Rev. Lett.* **110** 223603

[34] Vahala K J 2003 *Nature* **424** 839

[35] Lin G, Coillet A, and Chembo Y K 2017 *Adv. Opt. Photon.* **9** 828

[36] Dayan B, Parkins A S, Aoki T, Ostby E P, Vahala K J, and Kimble H J 2008 *Science* **319** 1062

[37] Junge C, O'Shea D, Volz J, and Rauschenbeutel A 2013 *Phys. Rev. Lett.* **110** 213604

[38] Reiserer A and Rempe G 2015 *Rev. Mod. Phys.* **87** 1379

[39] Ilchenko V S and Matsko A B 2006 *IEEE J. Sel. Top. Quantum Electron.* **12** 15

[40] Özdemir Ş K, Zhu J, Yang X, Peng B, Yilmaz H, He L, Monifi F, Huang S H, Long G L, and Yang L 2014 *Proc. Natl. Acad. Sci. USA* **111** E3836

[41] Li B B, Clements W R, Yu X C, Shi K, Gong Q, and Xiao Y F 2014 *Proc. Natl. Acad. Sci. USA* **111** 14657

[42] Foreman M R, Swaim J D, and Vollmer F 2015 *Adv. Opt. Photon.* **7** 168

[43] Chen W J, Özdemir Ş K, Zhao G M, Wiersig J, and Yang L 2017 *Nature* **548** 192

[44] Braginsky V B, Gorodetsky M L, and Ilchenko V S 1989 *Phys. Lett. A* **137** 393

[45] Kippenberg T J, Spillane S M, and Vahala K J 2004 *Phys. Rev. Lett.* **93** 083904

[46] Spillane S M, Kippenberg T J, and Vahala K J 2002 *Nature* **415** 621

[47] Yang Q F, Yi X, Yang K Y, and Vahala K 2017 *Nat. Photon.* **11** 560

[48] Guo H, Karpov M, Lucas E, Kordts A, Pfeiffer M H P, Brasch V, Lihachev G, Lobanov V E, Gorodetsky M L, and Kippenberg T J 2017 *Nat. Phys.* **13** 94

[49] Guo X, Zou C L, Jung H, and Tang H X 2016 *Phys. Rev. Lett.* **117** 123902

[50] Li Q, Davanço M, and Srinivasan K 2016 *Nat. Photon.* **10** 406

[51] Cao Q T, Wang H, Dong C H, Jing H, Liu R S, Chen X, Ge L, Gong Q, and Xiao Y F 2017 *Phys. Rev. Lett.* **118** 033901

[52] Jiao Y F, Lu T X, and Jing H 2018 *Phys. Rev. A* **97** 013843

[53] Post E J 1967 *Rev. Mod. Phys.* **39** 475

[54] Chow W W, Gea-Banacloche J, Pedrotti L M, Sanders V E, Schleich W, and Scully M O 1985 *Rev. Mod. Phys.* **57** 61

[55] Ciminelli C, Dell'Olio F, Campanella C E, and Armenise M N 2010 *Adv. Opt. Photon.* **2** 370

[56] Ge L, Sarma R, and Cao H 2014 *Phys. Rev. A* **90** 013809

[57] Li B, Özdemir Ş K, Xu X W, Zhang L, Kuang L M, and Jing H 2021 *Phys. Rev. A* **103** 053522

[58] Sarma R, Ge L, Wiersig J, and Cao H 2015 *Phys. Rev. Lett.* **114** 053903

[59] Zhang H L, Peng M Y, Xu X W, and Jing H 2022 *Chin. Phys. B* **31** 014215

[60] Maayani S, Dahan R, Kligerman Y, Moses E, Hassan A U, Jing H, Nori F, Christodoulides D N, and Carmon T 2018 *Nature* **558** 569

[61] Jiang Y, Maayani S, Carmon T, Nori F, and Jing H 2018 *Phys. Rev. Appl.* **10** 064037

[62] Jing H, Lü H, Özdemir S K, Carmon T, and Nori F 2018 *Optica* **5** 1424

[63] Zhang H L, Huang R, Zhang S D, Li Y, Qiu C W, Nori F, and Jing H 2020 *Nano Lett.* **20** 7594

[64] Huang R, Miranowicz A, Liao J Q, Nori F, and Jing H 2018 *Phys. Rev. Lett.* **121** 153601

[65] Li B J, Huang R, Xu X W, Miranowicz A, and Jing H 2019 *Photon. Res.* **7** 630

[66] Xu X W, Zhao Y J, Wang H, Jing H, and Chen A X 2020 *Photon. Res.* **8** 143

[67] Xu X W, Li Y, Li B J, Jing H, and Chen A X 2020 *Phys. Rev. Appl.* **13** 044070

[68] Jiao Y F, Zhang S D, Zhang Y L, Miranowicz A, Kuang L M, and Jing H 2020 *Phys. Rev. Lett.* **125** 143605

[69] Davuluri S and Zhu S 2015 *Europhys. Lett.* **112** 64002

[70] Lü H, Jiang Y, Wang Y Z, and Jing H 2017 *Photon. Res.* **5** 367

[71] Mirza I M, Ge W, and Jing H 2019 *Opt. Express* **27** 25515

[72] Boyd R W 2008 *Nonlinear Optics* (New York: Academic Press)

[73] Malykin G B 2000 *Phys. Usp.* **43** 1229

[74] Gardiner C W and Collett M J 1985 *Phys. Rev. A* **31** 3761

[75] Adair R, Chase L L, and Payne S A 1989 *Phys. Rev. B* **39** 3337

[76] Reimann R, Doderer M, Hebestreit E, Diehl R, Frimmer M, Windey D, Tebbenjohanns F, and Novotny L 2018 *Phys. Rev. Lett.* **121** 033602

[77] Ahn J, Xu Z, Bang J, Deng Y H, Hoang T M, Han Q, Ma R M, and Li T 2018 *Phys. Rev. Lett.* **121** 033603

[78] Maayani S, Martin L L, Kaminski S, and Carmon T 2016 *Optica* **3** 552

[79] Sofikitis D, Bougas L, Katsoprinakis G E, Spiliotis A K, Loppinet B, and Rakitzis T P 2014 *Nature* **514** 76

[80] Xu H, Mason D, Jiang L, and Harris J G E 2016 *Nature* **537** 80

[81] Ruesink F, Miri M A, Alù A, and Verhagen E 2016 *Nat. Commun.* **7** 13662